plate and an electrode. The mounting plate is lifted up over the substrate by a specially-designed drawbridge structure developed in our previous work [4]. The mounting plate is designed to have a large area (612×300 μm), therefore the required driving voltage can be low. Two fibres are aligned using translation stages and then fixed to the substrate by use of a strong adhesive. The distances between the fibre terminals and the micromirror are both 10 μm.

Initially, the micromirror is kept away from the light path, and the light beam from the input fibre passes to the output fibre with a small attenuation, corresponding to the insertion loss of the VOA. It is measured to be 1.5 dB at 1.55 μm wavelength. When the driving voltage applied to the actuator increases from 0 to 8 V, the mirror gradually moves down so that it cuts into the light path and blocks a portion of the light energy. As a result, the light intensity is attenuated. The attenuation can continuously increase to 45 dB as shown in Fig. 2. Further increase of the driving voltage does not produce higher attenuation as the signal power becomes too weak to be detected in our experiment.

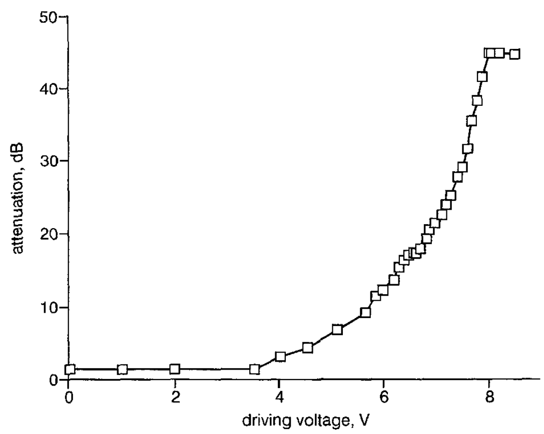

Fig. 2 *Static relationship of driving voltage and attenuation of MEMS VOA at 1.55 μm wavelength*

Dynamic response of the MEMS VOA is shown in Fig. 3. A square wave signal of 4 Hz repetition rate and 0 to 8 V voltage is applied to the actuator. The power coupled to the output fibre was measured to range from 71 to 0.003%, corresponding to an attenuation of 1.5 to 45 dB, respectively. The 0–90% rise time ($0 \rightarrow 8$ V) is measured to be 37 ms, and the 100–10% fall time is 36.4 ms. The rise and fall times are nearly identical.

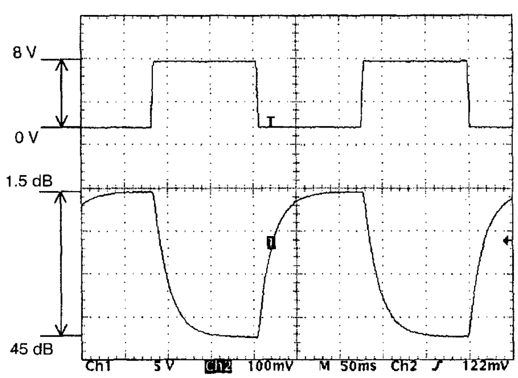

Fig. 3 *Dynamic response of MEMS VOA*

Several attenuation spectra measured in the MEMS VOA over the wavelength range 1520–1620 nm are shown in Fig. 4. The attenuation variation (i.e. wavelength dependence loss) is about 2.4 dB over the whole range, and less than 0.9 dB over the C-band (1528–1561 nm). Although MEMS components are expected to have small wavelength dependence, this is only true when the light beam is operated by the reflection of the MEMS mirror. In the MEMS VOA, the near-field diffraction plays a role. It determines the light that propagates to the output fibre, especially when the beam is partially blocked by the mirror. As a result, the attenuation becomes slightly wavelength dependent.

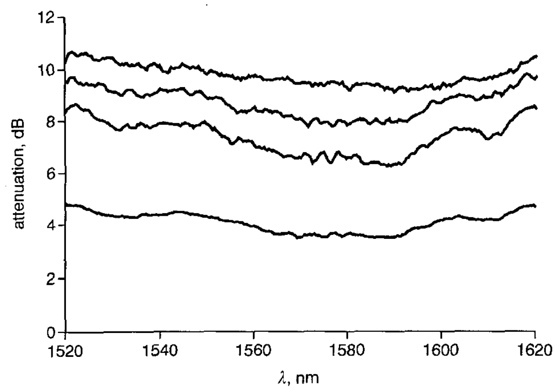

Fig. 4 *Wavelength dependence of attenuation*

Conclusions: A MEMS variable optical attenuator using the proprietary micromachined drawbridge structure is described. The device requires only 8 V driving voltage. It has 45 dB dynamic range of attenuation and 37 ms response time. The insertion loss of the device is 1.5 dB, and over the C-band it has less than 0.9 dB wavelength dependence loss.

12 December 2001
Electronics Letters Online No: 20020262
DOI: 10.1049/el:20020262

X.M. Zhang, A.Q. Liu, C. Lu and D.Y. Tang (*School of Electrical and Electronic Engineering, Nanyang Technological University, Nanyang Avenue, 639798 Singapore*)

E-mail: eaqliu@ntu.edu.sg

References

1 FORD, J.E., WALKER, J.A., GREYWALL, D.S., and GOOSSEN, K.W.: 'Micromechanical fiber-optic attenuator with 3 μs response', *J. Lightwave Technol.*, 1998, **16**, (9), pp. 1663–1670

2 MARXER, C., GRISS, P., and DE ROOIJ, N.F.: 'A variable optical attenuator based on silicon micromechanics: ', *IEEE Photonics Technol. Lett.*, 1999, **11**, (2), pp. 233–235

3 GILES, C.R., AKSYUK, V., BARBER, B., RUEL, R., STULZ, L., and BISHOP, D.: 'A silicon MEMS optical switch attenuator and its use in lightwave subsystems', *IEEE J. Sel. Top. Quantum Electron.*, 1999, **5**, (1), pp. 18–25

4 LIU, A.Q., ZHANG, X.M., MURUKESHAN, V.M., ZHANG, Q.X., ZOU, Q.B., and UPPILI, S.: 'Optical switch using draw-bridge micromirror for large array crossconnects'. 11th Int. Conf. on Solid-State Sensors and Actuators (Transducer '01 Eurosensors XV), Munich, Germany, 10–14 June 2001, pp. 1314–1317

Channel estimation and interference suppression in frequency-selective fading channels

Hongbin Li, Ling Li and Yu-Dong Yao

The issue of interference suppression is considered for wireless time-division multiple-access (TDMA) systems equipped with multiple receive antennas in frequency-selective fading channels. A novel scheme is presented to estimate the multipath channel, coherently demodulate information symbols, and meanwhile suppress radio interference. The proposed scheme is simple to implement and able to mitigate interference of various origins, including inter-symbol interference, co-channel interference and others. Numerical examples are presented to illustrate the performance of the proposed scheme.

Introduction: Wireless cellular systems are known to suffer from various sources of interference, such as co-channel interference (CCI) due to frequency-reuse and inter-symbol interference (ISI) caused by multipath propagation. Several interference reduction and equalisation techniques have been proposed in the past. For example, joint detection of all co-channel signals [1, 2] was found to yield excellent performance at the cost of computational complexity. In particular, the complexity of optimum joint demodulation increases exponentially as the number of users increases [3]. A second approach is through channel coding, which exploits time diversity and trades bandwidth for interference cancellation [4, 5]. When multiple antennas are affordable, spatial diversity can be used to effectively suppress interference without bandwidth expansion [6, 7]. It was shown that when optimum combining is applied, N_r receive antennas can be used to null out $N_r - 1$ interferers in flat-Rayleigh fading channels [6].

The optimum combining/processing schemes considered in [6, 7] require the channel state information (CSI) for *all* co-channel users, which may be difficult to obtain. In this Letter, we propose an alternative scheme that also makes use of spatial diversity for interference cancellation in frequency-selective channels. The proposed scheme is simple to implement. Although it is suboptimal in general, the proposed scheme is effective in mitigating interference of various sources, including ISI, CCI, and others.

Problem formulation: Consider a wireless cellular system that is equipped with N_r receive antennas and operates in a frequency-selective fading environment. The discrete-time baseband multi-channels between the transmitter and receivers are modelled as finite duration impulse response (FIR) filters: $\{\mathbf{h}_l\}_{l=0}^{L}$, where L denotes an upper-bound of the filter order and $\mathbf{h}_l := [h_1(l), \ldots, h_{N_r}(l)]^T$, with $\{h_{n_r}(l)\}_{l=0}^{L}$ being the overall impulse response between the transmitter and the n_rth receiver, which combines the effect of the transmit/receive filters and physical channel and is sampled at the symbol rate. The channels are assumed to experience block-static fading, i.e. $\{h_{n_r}(l)\}$ remain (approximately) constant within a block and vary from block to block, to emulate, e.g. framed transmission in TDMA. Let $\{s(n)\}$ be the transmitted symbol stream and $\mathbf{y}(n) := [y_1(n), \ldots, y_{N_r}(n)]^T$ be formed from outputs of the N_r receivers sampled at the symbol rate. Then, we have

$$\mathbf{y}(n) = \sum_{l=0}^{L} \mathbf{h}_l s(n-l) + \mathbf{w}(n) = \mathbf{H}\mathbf{s}(n) + \mathbf{w}(n) \qquad n = 0, \ldots, N-1 \quad (1)$$

where $\mathbf{H} := [\mathbf{h}_0, \ldots, \mathbf{h}_L]$, $\mathbf{s}(n) := [s(n), \ldots, s(n-L)]^T$, and $\mathbf{w}(n) \in \mathcal{C}^{N_r \times 1}$ is composed of channel noise and interference (e.g. CCI). Assume that pilots are embedded in the transmission and, without loss of generality, the first M transmitted symbols $\{s(n)\}_{n=0}^{M-1}$ are pilots. The problem of interest is to estimate the channels $\{\mathbf{h}_l\}_{l=0}^{L}$, demodulate coherently the symbols $\{s(n)\}_{n=M}^{N-1}$, and in the mean time suppress any possible interference contained in $\mathbf{w}(n)$.

Proposed method: Although the exact distribution of $\mathbf{w}(n)$ is difficult to determine, we model it here as a complex Gaussian vector with zero mean and $E\{\mathbf{w}(n_1)\mathbf{w}^H(n_2)\} = \mathbf{Q}\delta(n_1 - n_2)$, where $\mathbf{Q} \in \mathcal{C}^{N_r \times N_r}$ denotes the *unknown* spatial covariance matrix and $\delta(n)$ is the Kronecker delta function. It will be shown that this assumption admits a simple and yet effective solution to the problem of interest.

Let $\mathbf{Y}_M := [\mathbf{y}_0, \ldots, \mathbf{y}_{M-1}]$ and $\mathbf{S}_M := [\mathbf{s}_0, \ldots, \mathbf{s}_{M-1}]$. It follows from the aforementioned assumption that the log-likelihood function of $\{\mathbf{y}(n)\}_{n=0}^{M-1}$ is proportional to (within an additive constant): $-\ln|\mathbf{Q}| - M^{-1}\,\mathrm{tr}\{\mathbf{Q}^{-1}(\mathbf{y}_M - \mathbf{H}\mathbf{S}_M)(\mathbf{y}_M - \mathbf{H}\mathbf{S}_M)^H\}$. Maximising this likelihood function yields the ML (maximum likelihood) estimates of the channel $\mathbf{H}$ and the spatial noise/interference covariance matrix $\mathbf{Q}$:

$$\hat{\mathbf{H}} = \hat{\mathbf{R}}_{sy}^H \hat{\mathbf{R}}_{ss}^{-1}, \qquad \hat{\mathbf{Q}} = \hat{\mathbf{R}}_{yy} - \hat{\mathbf{R}}_{sy}^H \hat{\mathbf{R}}_{ss}^{-1} \hat{\mathbf{R}}_{sy} \quad (2)$$

where $\hat{\mathbf{R}}_{yy} = M^{-1}\mathbf{Y}_M\mathbf{Y}_M^H$, $\hat{\mathbf{R}}_{ss} = M^{-1}\mathbf{S}_M\mathbf{S}_M^H$, and $\hat{\mathbf{R}}_{sy} = M^{-1}\mathbf{S}_M\mathbf{Y}_M^H$. The above ML estimates that $\hat{\mathbf{R}}_{ss}$ is invertible, which can be satisfied by choosing appropriate pilot symbols and $M \geq N_r$.

The information symbols, i.e. $\{s(n)\}_{n=M}^{N-1}$ [cf. (1)], are demodulated next. Using the ML parameter estimates obtained in (2), we henceforth assume that $\mathbf{H}$ and $\mathbf{Q}$ are known during demodulation. While an ML detector can be straightforwardly formulated, it will incur an exponential complexity as the frame length increases and, hence, has limited practical use. We will instead focus on linear detectors. Specifically, we consider a Markov-like linear detector [8] as follows.

The data received after pilot transmission are denoted by $\{\mathbf{y}(n)\}_{n=M}^{N-1}$, from which we form non-overlapping data vectors of length K, $\mathbf{y}_K(i) := [\mathbf{y}^T(iK+M), \ldots, \mathbf{y}^T(iK+K+M-1)]^T$, $i = 0, \ldots, I-1$, where

$$I = \left\lceil \frac{N-M}{K} \right\rceil$$

with $\lceil \cdot \rceil$ denoting the smallest integer greater than the argument. The choice of the sub-frame length K is made by a trade-off between performance and complexity: a larger K may lead to a better performance but at the cost of an increased complexity (e.g. [8]). Let $\mathbf{s}_K(i) := [s(iK+M-L), \ldots, s(iK+K+M-1)]$ and $\mathbf{w}_K(i) := [\mathbf{w}^T(iK+M), \ldots, \mathbf{w}^T(iK+K+M-1)]$. We then have

$$\mathbf{y}_K(i) = \mathcal{H}_K \mathbf{s}_K(i) + \mathbf{w}_K(i), \qquad i = 0, \ldots, I-1 \quad (3)$$

where $\mathcal{H}_K$ denotes the $KN_r \times (L+K)$ block-Toeplitz convolutional matrix:

$$\mathcal{H}_K = \begin{bmatrix} \mathbf{h}_L & \cdots & \mathbf{h}_0 & & \mathbf{0} \\ & \ddots & \ddots & \ddots & \\ \mathbf{0} & & \mathbf{h}_L & \cdots & \mathbf{h}_0 \end{bmatrix}$$

Note that using the previous assumption, $\mathbf{w}_K(i)$ is Gaussian with zero-mean and covariance matrix $\mathbf{I}_K \otimes \mathbf{Q}$. It follows from (3) that the (soft) Markov-like estimate of $\mathbf{s}_K(i)$ is given by

$$\hat{\mathbf{s}}_K(i) = [\mathcal{H}_K^H(\mathbf{I}_K \otimes \mathbf{Q}^{-1})\mathcal{H}_K]^{-1}\mathcal{H}_K^H(\mathbf{I}_K \otimes \mathbf{Q}^{-1})\mathbf{y}_K(i) \quad (4)$$

The estimates of the overlapping symbols in two consecutive frames due to Markov-like detection are obtained by taking an arithmetic average of the corresponding symbols. The final (hard) estimate of any element of $\mathbf{s}_K(i)$ is determined as the constellation point that is closest (in Euclidean distance) to the corresponding element of $\hat{\mathbf{s}}_K(i)$. This reduces to, for example, $\mathrm{sign}\{\Re(\hat{\mathbf{s}}_K(i))\}$ for binary phase shift keying (BPSK) constellation.

Remark: The Markov-like detector given by (4) can be viewed as a joint processor (i.e. equaliser, demodulator and interference suppressor). Since $\mathbf{w}_K(i)$ is not modelled exactly, it may contain other unmodelled interference (in addition to CCI) and the *overall* interference is suppressed by the joint processor.

Direct evaluation of (4) is computationally inefficient and thus not recommended, particularly when the subframe size K is large. However, the structure of $\mathcal{H}_K$ and $\mathbf{I}_K \otimes \mathbf{Q}^{-1}$ can be utilised to reduce the complexity significantly. We first note that

$$\mathcal{H}_K^H(\mathbf{I}_K \otimes \mathbf{Q}^{-1}) = \begin{bmatrix} \mathbf{Q}^{-1}\mathbf{h}_L & \cdots & \mathbf{Q}^{-1}\mathbf{h}_0 & & \mathbf{0} \\ & \ddots & \ddots & \ddots & \\ \mathbf{0} & & \mathbf{Q}^{-1}\mathbf{h}_L & \cdots & \mathbf{Q}^{-1}\mathbf{h}_0 \end{bmatrix}^H$$

which breaks down to the calculation of $L+1$ matrix-vector products of reduced dimension: $\{\mathbf{Q}^{-1}\mathbf{h}_l\}_{l=0}^{L}$. Let $\mathbf{\Phi} := \mathcal{H}_K^H(\mathbf{I}_K \otimes \mathbf{Q}^{-1})\mathcal{H}_K \in \mathcal{C}^{(K+L)\times(K+L)}$ and ϕ_{mn} denote its mnth element. Since $\mathbf{\Phi}$ is Hermitian symmetric, only the elements on and above the diagonal, i.e. ϕ_{mn} for $n \geq m$, need to be evaluated. Furthermore, it can be verified by direct calculation that ϕ_{mn} for $n \geq m$ is given by

$$\phi_{mn} = \begin{cases} \sum_{i=1}^{m} \mathbf{h}_{L-i+1}^H \mathbf{Q}^{-1} \mathbf{h}_{L-i+(m-n+1)} & 1 \leq m \leq L+1;\ m \leq n \leq m+L \\ \sum_{i=1}^{L+1} \mathbf{h}_{L-i+1}^H \mathbf{Q}^{-1} \mathbf{h}_{L-i+(m-n+1)} & L+2 \leq m \leq K;\ m \leq n \leq m+L \\ \sum_{i=1}^{L+K-m+1} \mathbf{h}_{i-1}^H \mathbf{Q}^{-1} \mathbf{h}_{i-1+(m-n)} & K+1 \leq m \leq K+L;\ m \leq n \leq K+L \\ 0 & \text{otherwise} \end{cases} \quad (5)$$

where it was assumed that $K \geq L+1$ and $\mathbf{h}_i = \mathbf{0}$ for $i < 0$. We see from (5) that the calculation of $\mathbf{\Phi}$ reduces to a total of $(L+1)(L+2)/2$ quadratic terms $\{\mathbf{h}_i^H\mathbf{Q}^{-1}\mathbf{h}_j\}_{i,j=0}^{L}$ and their combinations [note that

$\mathbf{h}_i^H\mathbf{Q}^{-1}\mathbf{h}_j = (\mathbf{h}_j^H\mathbf{Q}^{-1}\mathbf{h}_i)^H$], and thus can be easily carried out. Then the inverse of $(K+L)(K+L)$ matrix $\mathcal{H}_K^H(I_K \otimes \mathbf{Q}^{-1})\mathcal{H}_K$ is calculated.

Numerical examples: We consider a TDMA system with a quaternary phase shift keying (QPSK) constellation and $N_r = 4$ receive antennas. Following a Rayleigh-fading assumption, the channel coefficients $\{h_{n_r}(l)\}$ are generated as Gaussian random variables with zero mean and equal variance which are independent for different n_r and/or l; also, $\{h_{n_r}(l)\}$ are fixed within one frame and changed independently from frame to frame. In the following examples, we set $L = 1$ (a 2-ray channel), $N = 162$ (frame length), $M = 18$ (number of pilots within a frame), $K = 18$ (sub-frame size for detection), and the system is assumed to have one co-channel interferer, which is generated using a similar method to the desired user. We compare the proposed scheme with linear zero-forcing (ZF) and minimum mean-squared error (MMSE) receivers. The ZF and MMSE receivers are implemented as follows: first a channel estimate for the desired user is obtained via a least-squares (LS) fitting using the pilot symbols; the LS channel estimates are next substituted in the standard linear ZF and MMSE receivers for symbol demodulation. Note that with only the CSI of the desired user, the ZF receiver is able to suppress ISI, but not CCI.

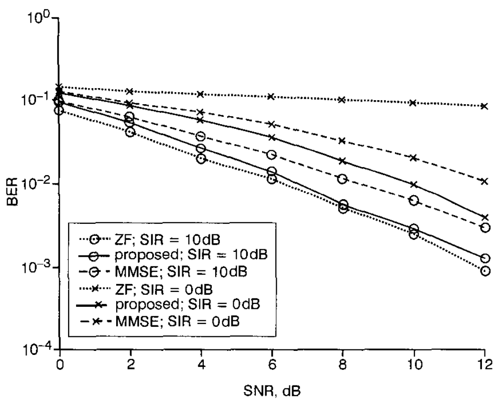

Fig. 1 *BER against SNR in Rayleigh fading channels*

Fig. 1 shows the bit error rate (BER) of the ZF and MMSE receivers as well as the proposed scheme against signal-to-noise ratio (SNR) under several values of signal to co-channel interference ratio (SIR). It is seen that when the CCI is weak, i.e. SIR = 10 dB, the ZF receiver performs best since it completely removes the ISI that dominates the overall interference in this case, and the proposed algorithm can achieve almost identical performance. When the CCI becomes stronger, i.e. for SIR = 0 dB, the ZF fails because it is unable to cope with CCI. However, the MMSE and the proposed receivers can better mitigate the overall interference. Yet the proposed scheme outperforms the MMSE receiver considerably for all values of SNR and SIR considered in this example.

Conclusions: We have proposed a channel estimation and interference cancellation scheme for wireless cellular systems that utilises spatial diversity receiving. The proposed scheme is simple to implement and able to deal with interference of various sources. Therefore, it is effective and computationally efficient. While only spatial diversity is invoked in this Letter, the proposed scheme may be extended to incorporate time diversity techniques as discussed in [4, 5]. This will be investigated in the near future.

Acknowledgment: This work was supported by the New Jersey Center for Wireless Telecommunications (NJCWT).

12 December 2001
Electronics Letters Online No: 20020271
DOI: 10.1049/el:20020271

Hongbin Li, Ling Li and Yu-Dong Yao (*Department of Electrical and Computer Engineering, Stevens Institute of Technology, Castle Point on Hudson, Hoboken, NJ 07030, USA*)

E-mail: hli@stevens-tech.edu

References

1 WALES, S.W.: 'Techniques for cochannel interference suppression in TDMA mobile radio systems', *IEE Proc., Commun.*, 1995, **142**, pp. 106–114

2 ARSLAN, H., and MOLNAR, K.: 'Cochannel interference suppression with successive cancellation in narrow-band systems', *IEEE Commun. Lett.*, 1998, **5**, pp. 37–39

3 VERDÚ, S.: 'Multiuser detection' (Cambridge Press, New York, NY, 1998, 1st edn.)

4 SESHADRI, N., CALDERBANK, A.R., and POTTIE, G.: 'Channel coding for co-channel interference suppression in wireless communications'. Proc. of the 1995 IEEE International Conference on Communications (ICC'95), 1995, pp. 884–888

5 CALDERBANK, A.R., POTTIE, G., and SESHADRI, N.: 'Cochannel interference suppression through time/space diversity', *IEEE Trans. Inform. Theory*, 2000, **46**, pp. 922–932

6 WINTERS, J.H., SALZ, J., and GITLIN, R.D.: 'The impact of antenna diversity on the capacity of wireless communication systems', *IEEE Trans. Commun.*, 1994, **42**, pp. 1740–1751

7 LI, Y.G.: 'Spatial-temporal processing for wireless mobile systems with ISI and CCI'. Proc. of the WCC-ICCT 2000, 2000, vol. 2, pp. 172–179

8 SÖDERSTRÖM, T., and STOICA, P.: 'System identification' (Prentice Hall International, London, UK, 1989)

Effect of constrained fast power control on cellular DS-CDMA systems with base station diversity

J.M. Romero Jerez, M. Ruiz García and A. Díaz Estrella

An approach is presented for determining the effect of limiting the power transmitted by a mobile user in a cellular DS-CDMA system with fast power control under multipath fading. It is shown that the system capacity can be increased if very deep fades are not compensated.

Introduction: Fast power control in CDMA systems can increase the capacity by eliminating fluctuations in the received signal. Perfect power control that tracks multipath fading requires the transmission of very high power levels occasionally when the user is in a deep fade, which increases the intercell interference. However, in real systems, the transmitted power of the mobile is necessarily limited. Analytical results for the performance of cellular CDMA system with fast power control under multipath fading has been recently presented, but, to simplify the analysis, it is commonly assumed that users connect to the nearest base station [1, 2]. However, in reality, the mobile is usually connected to the most favourable among a set of base stations.

System model: We consider the uplink channel of a cellular DS-CDMA system with N users per cell. Each user communicates with the base station that provides the least average attenuation among a set of N_c closest base stations. Therefore, the area of the system will be divided in two regions: the region R_0, which contains the points having the reference base station BS_0 among the N_c nearest base stations; and the region R_1, which contains the points not having BS_0 among the N_c nearest base stations.

The radio channel is affected by distance, path-loss exponent, lognormal shadowing and multipath fading. Fast power control is employed and the power transmitted by a mobile user to compensate multipath fading is limited to a given value P_M. We consider that M equal strength signals with Rayleigh distribution are received and optimally combined in RAKE receivers. The power of the multipath fading will thus have a chi-squared distribution with $2M$ degrees of freedom, with a probability density function given by:

$$f_{\chi_F}(x) = \frac{M^M}{(M-1)!} x^{M-1} e^{-Mx} \quad (1)$$

Probability of outage calculation: With direct sequence BPSK of spreading bandwidth W and assuming a sinc chip shape, the following expression holds for the ratio of despread bit energy to interference